

First evidence for a new spontaneous fission decay produced in the reaction $^{30}\text{Si} + ^{238}\text{U}$

H. Ikezoe¹, T. Ikuta¹, S. Mitsuoka¹, Y. Nagame¹, I. Nishinaka¹, K. Tsukada¹, T. Ohtsuki², T. Kuzumaki², J. Lu^{1,3}

¹ Japan Atomic Energy Research Institute, Tokai-mura, Naka-gun, Ibaraki-ken, 319-11 Japan

² Laboratory of Nuclear Science, Tohoku University, Mikamine, Taihaku-ku, Sendai 982, Japan

³ Institute of Modern Physics, Chinese Academy of Sciences, 73000 Lanzhou, China

Received: 13 March 1998 / Revised version: 4 May 1998

Communicated by V. Metag

Abstract. The first evidence for a new spontaneous fission decay has been observed in the evaporation residues for the reaction $^{30}\text{Si} + ^{238}\text{U}$ at the bombarding energy of 158 MeV. The measured half-life is 54_{-21}^{+98} s and the production cross section is 180_{-120}^{+240} pb. The observed spontaneous fission decay is a possible candidate for the spontaneous fission decay of ^{264}Sg or ^{263}Db after the β -decay of ^{263}Sg .

PACS. 23.90.+w Other topics in radioactive decay and in-beam spectroscopy – 25.70.-Z Low and intermediate energy heavy ion reactions – 27.90.+b $220 \leq A$

The spontaneous fission half-lives of heavy even-even nuclei decrease with increasing the atomic number Z up to 104. Recently the heavy seaborgium isotopes $^{265,266}\text{Sg}$ have been synthesized in the heavy-ion fusion reactions at Dubna [1] and GSI [2]. These isotopes mainly decay by emitting α -particles. This fact indicates that the nuclear stability against fission caused by nuclear shell structure increases significantly near the neutron number 162. In order to study the decay property of the heavy elements ($Z \geq 106$), an effort was made to synthesize a new seaborgium isotope ^{264}Sg in the reaction $^{30}\text{Si} + ^{238}\text{U}$.

Beams of ^{30}Si delivered from the JAERI-tandem accelerator were used to bombard a $^{nat}\text{UF}_4$ target whose thickness was $580 \mu\text{g}/\text{cm}^2$. The target was prepared by evaporation of the UF_4 material onto a $1.5 \mu\text{m}$ aluminium semicircular backing and mounted on a target wheel of 140 mm diameter. The target wheel was rotated with 2 cycles per second. Reaction products emitted from the target foil were separated in-flight from the primary beam and products of various background reactions by the recoil mass separator (JAERI-RMS) [3].

The details of the detection method are shown elsewhere [4]. The reaction products were implanted in a double-sided position sensitive strip detector (PSSD) installed at the focal position of the JAERI-RMS. The PSSD (73 mm \times 55 mm, 15 strips in the front face and 128 strips in the back face) provided two-dimensional positions and energies associated with implanted reaction products and subsequent decays. The each strip in the front face was position sensitive in the horizontal direction and 128 strips were divided into 8 resistance chains to read out a vertical position within a group. The energy resolution was

80 keV (FWHM) for the α -particle energy of 5.486 MeV from an ^{241}Am source. The PSSD was surrounded by four solid state detectors (60 mm \times 60 mm) to detect escaped α -particles and one of a pair of fission fragments following the decays of the implanted reaction products in the PSSD. A microchannel plate detector (MCP) was installed at 290 mm upstream from the PSSD and a flight time of each reaction product passing through the JAERI-RMS was measured between the MCP and the PSSD to give the mass discrimination.

The measured energies for heavy reaction products were corrected with the pulse height defect using the equation of [5]. The pulse height defect of the PSSD was measured by detecting the ^{238}U recoil of 56.3 MeV corrected with the energy loss of 6.3 MeV in the target at the present bombarding energy of 157.6 MeV. A detector depending parameter in the equation was adjusted to reproduce the measured pulse height defect.

The bombarding energy of 157.6 MeV which was about 1 MeV lower than the Bass fusion barrier was chosen to correspond to the maximum of the $4n$ deexcitation channel which was calculated by the code HIVAP [6]. The beam intensity was about 100 pA and the total dose was 2.64×10^{17} particles. The JAERI-RMS was tuned to pass the ^{264}Sg recoil of the charge state 13^+ and the recoil energy 13.2 MeV. Since the JAERI-RMS could accept only one charge state of the recoil, it was important to correctly estimate the most probable charge state of the recoil, which was estimated by using the equation of [7]. The total counting rate of the implanted reaction products, which were mainly composed of low energy scattered beams and target-like products, was $2 \sim 3$ Hz.

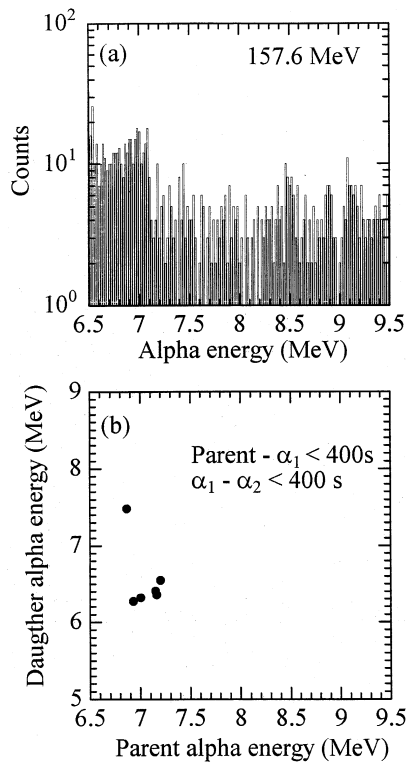


Fig. 1. **a** α spectrum for all decay events observed in the present reaction, **b** A two dimensional spectrum showing the correlation between parent and daughter α decays. the time gate of 400 s was set for the correlation between parent and daughter α_1 and also for the correlation between daughter α_1 and granddaughter α_2

The time-ordered data were sorted to identify correlated decay events within the position deviations of ± 0.4 mm for the horizontal direction and ± 0.5 mm for the vertical direction in the PSSD, where the position deviations are given with respect to the implantation site of the reaction product.

An α spectrum for all decay events observed is shown in Fig. 1a. It was difficult to discriminate completely light particles like α -particles passing through the JAERI-RMS from the true decay events associated with implanted reaction products, because the detection efficiency of the MCP was $60 \sim 70\%$ for α -particles. The α -decays associated with the heavy elements ($100 \leq Z \leq 106$) are expected in the energy region between 7.0 MeV and 9.5 MeV. No distinct energy peak is seen in Fig. 1a. The correlation between parent and daughter α -decays, parent- α_1 - α_2 , is shown in Fig. 1b, where a correlation time of 400 s was set for parent-daughter α_1 and daughter α_1 -granddaughter α_2 . The observed 6 decay chains were attributed to the α -decays of ^{214}Ac , ^{222m}Ac , $^{208,210,211}\text{Ra}$ from the measured time-energy correlations.

The α -decays from the heavy fusion residues ($Z \geq 100$) were not identified in the present analysis, while six fission decays correlated with implanted heavy reaction products ($A \geq 220$, where A is the mass number) were observed

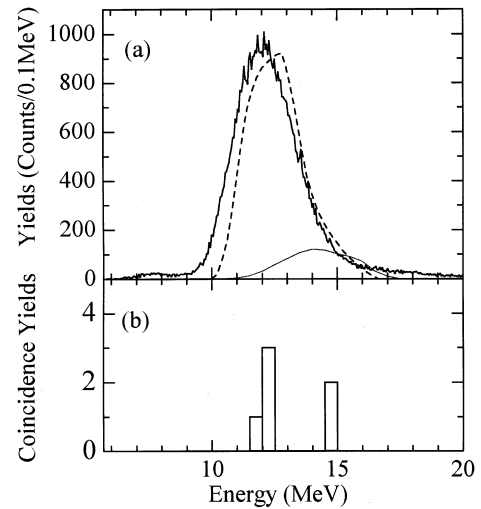


Fig. 2. **a** Measured energy spectrum (the solid line) of reaction products ($A \geq 180$). The calculated energy spectra for the ^{238}U recoil and the ^{264}Sg recoil are shown as the dashed line and the thin solid line, respectively, **b** The parent energy distribution corresponding to the observed six fission events

within the correlation time of 400 s. The observed energies E and A of these heavy reaction products are listed in Table 1 together with the energies E_f and the times t of the spontaneous fission fragments after the implantation of these heavy products. The fission decays were identified by detecting a large energy deposit ($E \geq 69$ MeV) in the PSSD and at the same time detecting the one of a pair of fission fragments in any one of the four detectors surrounding the PSSD. It should be noted that the four detectors were installed so that the incoming reaction products did not directly hit these detectors. The kinetic energies of the implanted reaction products correlated with these six fission decays were plotted in Fig. 2 together with the single energy spectrum of implanted reaction products ($A \geq 180$).

Since the mass and energy acceptances of the JAERI-RMS are $\pm 3.5\%$ and $\pm 12\%$, respectively, the target-like recoils of the charge state 12^+ and the energy around 12 MeV can also pass through the JAERI-RMS. The calculated energy distribution for the ^{238}U recoil passing through the JAERI-RMS is shown as the dashed line in Fig. 2a with an arbitrary normalization. The measured energy of the target-like products are slightly shifted towards the lower energy side compared with the calculated result. This difference is probably due to the contribution of lighter target-like products ($A < 238$) which are not taken into account in the calculation. The calculated energy distribution for ^{264}Sg is also shown in Fig. 2a as the thin solid line with an arbitrary normalization. In this calculation, the energy and the angular distributions of the $4n$ channel evaporation residue were calculated by using the statistical model code Pace2 [8]. The multiple scattering and the energy loss of the evaporation residue in the target were calculated by the code TRIM [9] and the

Table 1. Fission decay events correlated with implanted heavy reaction products ($A \geq 220$). E_f^0 and E_f are the fission fragment kinetic energies without and with the correction of the pulse height defect, respectively. The average counting rates of the heavy recoils passing through the JAERI-RMS are shown for two energy regions of the recoil energy in the column 10 and 11

SF events	Strip #		E (MeV)	A	E_f^0 (MeV)	E_f (MeV)	t (s)	N_f	Counting rate (10^{-3} cps)	
	n_x	n_y							$E < 14$ MeV	$E \geq 14$ MeV
1	8	6	14.9	253	87.5	97	51	6	40	5.1
2	9	5	14.6	241	84.8	94	105	1	45	3.1
3	6	6	12.0	235	105	114	162	2	10	1.0
4	8	6	12.1	254	68.6	78	131	6	40	5.1
5	9	4	11.8	228	87.0	95	40	2	38	4.2
6	12	2	12.2	255	93.1	103	8.4	2	1.5	0.2

beam transport efficiency of the evaporation residue was calculated by the code GIOS [10].

As shown in Fig. 2a, the calculated energy distributions for the ^{238}U recoil and the ^{264}Sg recoil are overlapped each other. Therefore, it is difficult to classify unambiguously the observed six recoils into the ^{238}U recoil or the ^{264}Sg recoil. However, as shown in Table 1, the measured mass numbers of the events No. 3 and 5 are inconsistent with the ^{264}Sg recoil and rather consistent with the ^{238}U recoil within the experimental error $\pm 10\%$. As the probability to observe a ^{264}Sg recoil at an energy of 12 ± 0.5 MeV is four times smaller than to observe it at an energy of 14 ± 0.5 MeV, it cannot be excluded that the events No. 4 and No. 6 are random coincidences with ^{238}U recoils. However, their mass numbers were consistent with ^{264}Sg recoils.

The possible fission background is considered to be the fission decay of ^{252}Cf , because the PSSD is contaminated by only a very small amount of ^{252}Cf . The probability of the random coincidence between the fission decay of ^{252}Cf and the implanted reaction products ($A \geq 180$) was estimated by taking into account the total numbers of fission events and the implanted reaction products and the total data acquisition time of about five days. The total numbers of background fission events N_f detected in a small rectangular portion of the PSSD specified by the strip number n_x in the horizontal direction and the group number n_y in the vertical direction are shown in Table 1 together with the average counting rate of the implanted reaction products. By taking into account the finite position resolution of the PSSD, the number of the random coincidence during the time interval of 100 s was estimated to be 0.28 and 0.08 for the low energy component ($E < 14$ MeV) and the high energy component ($E \geq 14$ MeV) of the implanted reaction products, respectively. This means that the error probability [11] is 3.2×10^{-3} for the two fission decays with the parent kinetic energy around 14.5 MeV. On the other hand, the fission decays with the parent kinetic energy around 12 MeV may contain some random coincidence events with target-like products.

From the above consideration, at least the two fission decays, the events No. 1 and No. 2, can be attributed to a spontaneous fission decay produced in the reaction $^{30}\text{Si} + ^{238}\text{U}$. The fission events of No. 4 and No. 6 can not

be completely excluded from the true coincidence event, while the fission events of No. 3 and No. 5 are probably originated from the random coincidence with target-like products.

The half-life and the production cross section of the two spontaneous fission events of No. 1 and No. 2 were 54_{-21}^{+98} s and 180_{-120}^{+240} pb, respectively. If the four fission events (No. 1, 2, 4, and 6) are taken into account, the half-life becomes 51_{-17}^{+51} s and the production cross section increases to 360_{-180}^{+270} pb. The cross section was evaluated using the calculated efficiency 3.7% of the JAERI-RMS.

Since any α -decay preceding to the fission decays was not observed within the time window of 400 s after implantation and the energy region between 1 MeV and 10 MeV, it is difficult to identify definitely the observed fission decays as the decay of ^{264}Sg . The nuclei ^{259}Lr , ^{263}Rf and $^{262,263}\text{Db}$ whose spontaneous fission half-life are close to the measured value, may be considered as a parent nucleus of the observed spontaneous fission decays in addition to ^{264}Sg . Among these, the nuclei $^{259}\text{Lr}(\alpha p 4n)$, $^{262}\text{Db}(p 5n)$ and $^{263}\text{Db}(p 4n)$ are scarcely produced in the present bombarding energy, because their calculated production cross sections are the two to three orders of magnitude smaller than the one for the $4n$ channel cross section. (The evaporation channels to produce these nuclei are indicated in each parenthesis.) Although the nucleus ^{263}Rf is the unknown isotope, its spontaneous fission half-life is reported to be 500_{-200}^{+300} s [12]. This nucleus can be produced in the αn and $2p3n$ channels. Even if the cross section of the $(HI, \alpha xn)$ reactions is about 3 - 5 times larger than those for the (HI, xn) reactions [13], the αn cross section is negligibly small in the present excitation energy 48 MeV compared with the $4n$ cross section. This is also true for the $2p3n$ channel cross section, because the cross section maximum for the $2p3n$ channel is located at the high excitation 62 MeV.

The nucleus ^{263}Sg can be produced with the same order of magnitude as the $4n$ cross section. The nucleus ^{263}Sg whose half-life is 0.8 s decays into ^{259}Rf by an α -decay with the branching ratio of 30 % and decays by a spontaneous fission with the branching ratio of 70 % [14]. In addition, the β -decay of the nucleus ^{263}Sg is theoretically predicted with the calculated half-life of 17.5 s

[15]. The daughter nucleus ^{263}Db whose half-life is 27 s decays by an α decay (43 %) and a spontaneous fission decay (57 %). Therefore, the nucleus ^{263}Sg becomes also the candidate in addition to the nucleus ^{264}Sg . The cross section for the $3n$ channel, which corresponds to the production of ^{265}Sg , was evaluated to be the one order of magnitude smaller than the cross section for the $4n$ channel in the present bombarding energy, because the cross section maximum for the $3n$ channel is well below the Bass barrier. The possibility to attribute the observed fission decays to the one of the long lived spontaneous fissions of ^{256}Cf (12.3 m), ^{256}Fm (157.6 m), ^{259}Md (96 m) and ^{261}Lr (39 m) is also small, because their decay probabilities for the time window 100 s are less than 0.1.

The obtained half-life is close to the fission half-life of ^{266}Sg [2] and the one order of magnitude larger than the calculated spontaneous fission half-life 2.3 s [16] for ^{264}Sg . The observed spontaneous fission decays are a possible candidate for the spontaneous fission decay of ^{264}Sg or ^{263}Db after the β -decay of ^{263}Sg .

The authors would like to thank the accelerator crew of JAERI tandem facility for the excellent performance of the accelerator.

References

1. Yu. A. Lazarev et al., *Phys. Rev. Lett.* 73, 624 (1994)
2. M. Schädel et al., *Nature* 388, 55 (1997) and M. Schädel et al., *Radiochim. Acta* 77, 149 (1997)
3. H. Ikezoe et al., *Nucl. Instr. and Meth.* A376, 420 (1996)
4. H. Ikezoe et al., *Phys. Rev.* C54, 2043 (1996)
5. S. B. Kaufman et al., *Nucl. Instr. and Meth.* 115, 47 (1974)
6. W. Reisdorf and M. Schädel, *Z. Phys.* A343, 47 (1992)
7. K. Shima et al., *Nucl. Instr. and Meth.* 200, 605 (1982)
8. A. Gavron, revised version of the code PACE; see *Phys. Rev.* C21, 230 (1980)
9. J. F. Ziegler and J. P. Biersack, a program for the calculation of the stopping and range of ions in solids, Pergamon Press, New York 1985
10. H. Wollnik et al., a program for the design of general ion-optical systems. Physikalisches Institut, Universität Giessen, D-6300 Giessen, Germany
11. K.-H. Schmidt et al., *Z. Phys.* A316, 19 (1984)
12. K. R. Czerwinski, Ph.D. Thesis, LBL-32233, (1992)
13. A. N. Andreyev, et al., *Z. Phys.* A345, 389 (1993)
14. Table of Isotopes edited by V. S. Shirley et al., A Wiley-Interscience Publication
15. P. Möller et al., *Atomic Data and Nuclear Data Tables* 66, 131 (1997)
16. R. Smolańczuk et al., *Phys. Rev.* C52, 1871 (1995)